Transcriptome and Proteome Analysis Reveals Corosolic Acid Inhibiting Bladder Cancer via Targeting Cell Cycle and Inducing Mitophagy *in Vitro* and *in Vivo*

Anfang Cui
Jining Medical University
Xiangling Li
Jining Medical University
Xiaolei Ma
Jining Medical University
Xiao Wang
Jining Medical University
Chang Liu
Jining Medical University
Zhigang Song
Jining Medical University
Feng Pan
Huazhong University of Science and Technology Tongji Medical College
Yong Xia (xiayong@mail.jnmc.edu.cn)
Jining Medical University https://orcid.org/0000-0002-1020-0263
Changlin Li
Jining Medical University

Research Article

Keywords: Corosolic acid (CA), Bladder cancer, Anti-cancer activity, Mitosis, Mitophagy

Posted Date: July 15th, 2021

DOI: https://doi.org/10.21203/rs.3.rs-705930/v1

Abstract

Background

Existing chemotherapy and radiotherapy methods have drawbacks such as high toxicity, high side effects, poor efficacy, and chemoresistance. Therefore, there is an urgent need to develop new anti-cancer drugs with low toxicity and high efficiency for cancer therapy and the prevention of recurrence. Corosolic acid (CA) is a medicine and food homologue and has many biological activities of health care. However, the anti-tumor effects and mechanism of CA in bladder cancer remain unexplored.

Methods

To study the anticancer effect of CA on bladder cancer cells, CCK8, EdU, high-content living cell imaging experiments were performed. And the mice model was used to verify the anticancer effect and toxicity for mice. To investigate the molecular mechanism of CA inhibition on bladder cancer cells, transcriptomics and proteomics were employed. To further verify the pharmacological mechanism, flow cytometry, RT-qPCR, western blotting and immunofluorescence staining experiments were performed, and the CA targeting molecules were analyzed in combination with our experimental and public clinical data.

Results

We found that CA inhibited bladder cancer cell proliferation in a concentration- and time-dependent manner. Xenograft experiments showed that CA inhibited the growth of subcutaneous tumors, and had no toxicity in mice. Integration of omics analysis revealed that low concentrations of CA inhibited bladder cancer cells proliferation via attenuating DNA synthesis by downregulating TOP2A and LIG1, and via diminishing mitosis by downregulating CCNA2, CCNB1, CDC20, and RRM2. High concentrations of CA induced cell death not through the apoptotic pathway but through triggering mitophagy pathway via upregulating SQSTM1/P62, NBR1, and UBB.

Conclusions

CA, a natural compound homologous to medicine and food, inhibits the mitosis of bladder cancer cells at low concentrations, and kills bladder cancer cells by inducing mitophagy at high concentrations. This study provides a comprehensive understanding of the pharmacological mechanism of CA inhibition in bladder cancer for the first time, which is helpful for the development of new anti-tumor drugs based on CA.

Background

Bladder cancer is one of the ten most common malignant tumors worldwide and the fourth most common malignancy in men [1]. Currently, there are 1.65 million cases of bladder cancer, with 550,000 new cases diagnosed each year [2]. The highest incidence of bladder cancer is observed in Europe, North America, Australia, New Zealand, and other developed countries and regions [2]. With the rise in the general and aging populations, the number of diagnosed bladder cancers will continue to increase in the future [2]. Depending on the severity of the stage and grade of bladder cancer, treatment options may include surgery (e.g., transurethral resection of bladder tumor; TURBT), Bacillus Calmette-Guerin (BCG), chemotherapy, or radiotherapy [1]. However, current treatment methods for bladder cancer still have several disadvantages. For example, after radical resection of bladder cancer, the quality of life and sexual function of patients are often seriously affected [1]. The combination of TURBT with BCG treatment has been used in clinical application for 40 years, but the mechanism of BCG treatment is unclear. This treatment fails in some patients due to adaptive immune resistance, and the recurrence rate within two years is 40–60% [3, 4]. Besides, BCG also has the potential risk of local or systemic infection complications and multi-system diseases [5–7]. Existing chemotherapy and radiotherapy methods also have drawbacks such as high toxicity, high side effects, poor efficacy, and chemoresistance [8]. Therefore, there is an urgent need to develop new anti-cancer drugs with low toxicity and high efficiency for bladder cancer therapy and the prevention of recurrence.

Anti-cancer phytochemicals, a type of medicinal and food homologous substances, have attracted the attention of scientists in the fields of pharmacology and oncology [9]. Many anti-cancer natural compounds derived from plant sources, such as resveratrol, camptothecin, capsaicin, and catechin, have been extensively studied [10, 11]. Moreover, paclitaxel and vincristine have been clinically applied as first-line drugs in cancer therapy [12, 13]. Corosolic acid (CA) is a pentacyclic triterpenoid that is found in kiwi, crape myrtle, loquat, and other plants. It has been discovered that CA has a variety of biological activities, including anti-oxidation, regulation of blood sugar levels, and anti-fungal and anti-tumor properties [14]. Owing to these benefits, CA has been widely used as a health food supplement [15, 16]. More importantly, due to its significant role in diabetes treatment, CA is known as "plant insulin" [17]. CA has been reported to inhibit certain protein tyrosine phosphatases to enhance insulin receptor β phosphorylation and stimulate glucose metabolism, which in turn decreases blood sugar levels [18].

In addition, recent progress has been made in anti-tumor studies involving CA. For instance, CA inhibits colorectal cancer cell growth by suppressing the PI3K/Akt/PKA signaling pathway through binding to the outer domain of HER3 and forming stable hydrogen bonds with Gly515, Arg444, Ser412, and Pro512 [19]. Moreover, Wang et al. reported that CA dose-dependently suppressed Y-79 retinoblastoma cell growth by blocking the cell cycle and inducing apoptosis by targeting maternal embryonic leucine zipper kinase (MELK) and forkhead box M1 (FoxM1) [20]. The anti-cancer function of CA in urinary system tumors has also been studied. CA has been found to inhibit TRAMP-C1 prostate cancer cell growth by decreasing the methylation level of nuclear factor erythroid 2-related factor 2 (Nrf2) promoter CpG sites, resulting in the upregulation of both mRNA and protein levels of Nrf2. In addition, CA can induce the expression of heme oxygenase-1 (HO-1) and NADH quinone oxidoreductase 1 (NQO1), suppressing the transformation of TRAMP-C1 cells [21]. However, the inhibitory effect of CA on bladder cancer and its underlying molecular

mechanism remains unknown. In the present study, using cell proliferation, colony formation, and DNA synthesis assays, we found that CA significantly inhibited bladder cancer cell growth and verified the anti-cancer efficacy of CA. Using transcriptome and proteome analysis, we revealed a panoramic view of the mechanism by which CA inhibits bladder cancer: CA does not induce apoptosis but represses DNA replication and mitosis via significant downregulation of cell multiplication-related molecules TOP2A, LIG1, CCNA2, CCNB1, and CDC20. Interestingly, high concentrations of CA can lead to cell death in bladder cancer cells through induction of mitophagy by upregulating NBR1, SQSTM1/P62, UBB, and LC3. This study provides a comprehensive insight into the anti-cancer effects, toxicology, and pharmacological mechanisms of CA, which would provide compelling support for the development of anti-tumor drugs based on CA.

Methods

Cell culture

Human bladder cancer cells lines SW780 and UM-UC-3 were obtained from ATCC and cultured in DMEM (Hyclone, 37°C, 5% CO2) containing 10% FBS (Hyclone), 100 units/ml penicillin (Gbico), and 100 μg/ml streptomycin (Gbico).

Dual fluorescence staining of living/dead cells

Calcein AM is able to stain living cells showing green fluorescence; propidium iodide (PI) is able to stain dead cells showing red fluorescence. The two fluorescence probes (Calcein AM/PI) were employed to detect the activity of cell lactase and the integrity of cell membrane respectively, thus reflecting the cell activity and cytotoxicity. This kit was purchased from Beyotime (China, Beijing, C2015S).

Transcriptome and proteomic tests

In transcriptome sequencing, three control sampls and three CA-treated samples (5×10^6 cells each sample) were cleaved with Trizol, and then library building and mRNA sequencing were performed in Novogene (Beijing, China). For proteome assay, three control and three CA-treated (1.2×10^7 cells each sample) were lyzed with BD lysis buffer (containing 8M, 0.1M NaHCO3, 0.2% SDS), and then determined by 6-label TMT mass spectrometry at Norogena (Norogena, Beijing, China).

RNA extraction and quantitative RT-PCR

Total RNA was extracted from cells with Trizol reagent (Roche), and reverse transcribed to cDNA using high capacity reverse transcription kit (TIANGEN Biotech, China). Quantitative real-time PCR was performed using SuperReal PreMix Color (SYBR Green) (TIANGEN, China). Relative mRNA levels were normalized to GAPDH expression levels. All primers used for the PCR are listed in Table 1.

Table 1
The primer sequences for realtime-PCR

Primer	quantitative RT-PCR primer
CCNA2	Forward: ATGTCACCGTTCCTCCTTG
	Reverse: GGGCATCTTCACGCTCTAT
CCNB1	Forward: GCAGTAAATGATGTGGATGC
	Reverse: CCTCAAGTTGTCTCAGATAAGC
LIG1	Forward: GGAAGAGCAGACCAAGCCTC
	Reverse: ATCCAGGGGTCCCTCAGC
TOP2A	Forward: AGTCGCTTTCAGGGTTCTTGA
	Reverse: TGCATATTTTCATTTACAGGCTGC

Western blot analysis

Proteins were extracted from cultured cells in cell lysis buffer (P0013, Beyotime, China) supplemented with 1 mM PMSF. Protein extracts were subjected to 10% SDS-polyacrylamide gel and blotted on PVDF membranes. Immunoblotting was performed using the following primary antibodies: CCNA2 (1:800, Proteintech, China 18202-1-AP), CCNB1 (1:1000, Proteintech, China, 55004-1-AP), RRM2 (1:1000, CST, USA, #65939) and GAPDH (1:2000, OriGene, USA, TA802519). The horseradish peroxidase (HRP)–conjugated secondary antibodies were purchased from Proteintech.

Cell activity measurement

According to manufacturer's instruction, the cell counting kit (CCK-8, C0037, Beyotime, China) reagent was added into each well diluted by DMEM medium and incubated for 1 hour. A blank control only contained DMEM media (without cells) and CCK8 solution. Subsequently, 100μL CCK reaction solution was transferred into a 96-well-plate in triplicate. The optical density was measured with a microplate reader (Perkin Elmer Ensight Microplate Reader, USA) at a wavelength of 450nm.

Measurement of DNA synthesis rate by EdU method

To detect effects of compounds on cell, proliferation examination is one of basic method to evaluate the antitumor activity. The rate of DNA synthesis can reflect the rate of cell proliferation. EdU (5-ethynyl-2'-deoxyuridine) is a thymidine analog which can be substituted for thymidine in DNA synthesis. We used the EdU-594 cell proliferation detection kit (C0078L, Beyotime, China) to examine the synthesis of DNA according to manufacturer's instruction. The results of the EdU staining were photographed by CellInsight CX7 High-Content Screening (HCS) platform (Thermo Scientific, US).

Flow cytometry for cell cycle and apoptosis test

To examine the effects of the CA on the cell cycle, flow cytometry was employed. The cells were harvested by trypsin digestion after treatment, and fixed in 70% cold ethanol (in PBS) overnight at 4°C. Then PI/RNase staining solution (#4087, cell signaling technology, USA) was added for 20 min (in dark) and the stained cells were tested and counted by flow cytometer. The cells for apoptosis analysis were harvested by trypsin treatment, and stained by Annexin V-FITC Early Apoptosis Detection Kit (C1062M, Beyotime, China) for 20 min in darkness. The stained cells were counted and recorded by flow cytometer (Beckman Coulter, USA).

Cell clone formation assay

Cell clone formation test is a powerful technique to detect cell proliferation ability or sensitivity to killing factors. Three hundred cells were cultured into 12-well plate. After incubation at 37°C with 5% CO2 for 12 h, different concentrations of CA was added and the cells were cultured for 12 days (change media and CA every 3 days). The cell clones were photographed under a microscope.

Immunofluorescencent Staining

Cells growing in 24-well plates were fixed in 4% paraformaldehyde, labeled with primary antibodies 2 h at 37°C, and then incubated with species-appropriate secondary antibodies at room temperature for 1 h. Nuclei were stained with DAPI, and images were collected using CellInsight CX7 High-Content Screening (HCS) platform (Thermo Scientific, US). The antibodies used in immunofluorescencent staining were listed as following: mouse anti-KIF11 (1:50, LSBIO, LS-B10258), rabbit anti-SQSTM1/p62 (1:50, SantaCruz, sc-28359), rabbit anti-LC3 (1:300, Proteintech, 14600-1-AP).

Immunohistochemical Staining

Immunohistochemistry was employed to detect biomarkers in the xenografted tumor of nude mice. The 10% formalin fixed blocks were cut into 4-μM slices and dehydrated. The endogenous peroxidase was inactivated by H_2O_2. The antigenic was repaired with citric acid solution, heating for 20 minutes. After being incubated with primary and secondary antibodies, the samples were developed with DAB solution (Solarbio, DA1015). After being re-dyed by hematoxylin, the slides were dehydrated and sealed. The antibodies used in immunofluorescencent staining were listed as following: Ki67 (1:300, Abcam, ab15580), CDC20 (1:150, Proteintech, 10252-1-AP).

Mitochondrial membrane potential detection

Mitophagy is accompanied by the attenuation of mitochondrial membrane potential. The effect of CA on the mitochondrial membrane potential of bladder cancer cells was detected by Mito-Tracker Red CMXRos kit (Beyotime, China, C1049B) according to the manufacturer's instructions.

Xenograft in nude mice

10 six-week-old BALB/C-nude mice were injected subcutaneous with 10^7 bladder cancer SW780 cells. When the tumor grew to 100mm^3, the mice were randomly divided into two groups with 5 mice in each group. The CA-treatment group was intraperitoneally injected once every 2 days at a dose of 8 mg/kg (CA

was first dissolved in DMSO and then dissolved in corn oil), while the control group was given DMSO and corn oil at the same volume at the same IP injection frequency. After administration, the tumor volume was measured every 2 days and the mice were weighed every 3 days. After 10 doses injection, the mice were sacrificed, and the subcutaneous tumors were taken, photographed and weighed, then fixed with 10% formalin, dehydrated and made into paraffin blocks for subsequent studies. At the time of sacrificing mice, blood was collected for routine blood measurement.

Statistical analysis

The data were analyzed using one-way ANOVA and analysis was performed using Microsoft Excel and/or GraphPad Prism. $P < 0.05$ was considered significant.

Results

Corosolic acid inhibited bladder cancer cell proliferation

Corosolic acid, also known as 2α-hydroxy ursolic acid, is known as a plant-resourced parainsulin due to its hypoglycemic function [18]. However, there are few investigations on the anti-cancer function of CA. In the present study, we provided multiple evidences suggesting that CA inhibited bladder cancer, through cell and animal experiments and multi-omics analysis. CCK8 kit was used to detect the inhibitory effects of CA against bladder cancer cells. As shown in Fig. 1B and 1C, bladder cancer cell growth was suppressed by CA in a dose-dependent manner. IC50 for SW780 and UM-UC-3 were 6.31 μg/ml and 7.25 μg/ml, respectively. Following treatment with CA, the morphological characteristics of the bladder cancer cells were changed: first, the cell intensity was decreased; second, the cells were wrinkled, and attachment became unstable (Fig. 1D and 1E). Because the proliferation marker Ki67 represents the percentage of highly proliferative tumor cells correlating with the S-phase fraction and mitosis, we detected Ki67 in CA-treated cells using a high-content cell imaging system. Figure 1F shows the representative image of Ki67 staining, and Fig. 1G shows the quantitative evaluation of the staining intensity analyzed by the cell imaging system. As shown in Fig. 1F and 1G, CA reduced the nuclear staining ratio of Ki67, indicating that CA inhibited bladder cancer cell proliferation. To study the time-dependent anti-cancer effect of CA, we incubated the bladder cancer cells SW780 and UM-UC-3 with CA for 24h, 48h, and 72h and recorded the cell activity and morphological alterations. As seen in Fig. 1H and 1I, 7.0 μg/ml of CA suppressed the growth of SW780 and UM-UC-3 cells in a time-dependent manner. Cell morphologies were gradually altered by prolonged treatment with CA (Fig. 1J and 1K): while 48h treatment caused changes in cell shape, 72h treatment caused the bladder cancer cells to lose their attachment and extension features. The above results indicate that CA can inhibit the proliferation of bladder cancer cells in a time- and dose-dependent manner, suggesting that CA may be a potential natural source compound for the treatment of bladder cancer.

Corosolic acid inhibited transplanted tumor in vivo

To investigate the anti-tumor effect of CA against bladder cancer as well as its toxicity and side effects, we employed a xenograft nude mouse model. As shown in Fig. 1A, subcutaneous tumor growth slowed down with 8 mg/kg of CA treatment. After the mice were administered with CA, the tumor volume and tumor weight significantly decreased (Fig. 2B and 2C); however, the mice's body weight did not change significantly (Fig. 2C). To study the effect of CA on tumor pathology, the tumor sections were analyzed by H&E staining and IHC staining for Ki67 (Fig. 2D and 2E). As shown in Fig. 2E, the proliferation marker Ki67 was significantly decreased in the CA-treated group, indicating that CA treatment inhibited the proliferation of transplanted bladder cancer cells in nude mice. The side effects of CA were estimated through routine blood examination and kidney, heart, and liver dissection. As shown in Fig. 4F, CA did not cause a change the mouse blood index; only the average erythrocyte hemoglobin content (MCH) was increased. As shown by the H&E staining data in Fig. 4G–4I, CA did not affect the structure and H&E staining characteristics of mouse kidney, heart, and liver. The above data suggest that CA is an effective anti-bladder cancer compound with low toxicity to mice.

Corosolic acid inhibited bladder cancer via suppression of DNA replication and mitosis-related pathways

Pharmacological analysis based on multi-omics measurement has become a powerful method for revealing pharmacological mechanisms. In order to explore the anti-cancer mechanisms of CA, we performed transcriptome and proteome analyses of CA-treated bladder cancer cells along with control cells. As shown in the volcano map in Fig. 3A, using "$p < 0.05$ and absolute" and "value of Log2FoldChange greater than 0" as the screening threshold, CA-treated cells exhibited 3304 upregulated and 2917 downregulated transcripts. GO enrichment analysis of the differential transcripts revealed that the altered transcripts were enriched in DNA synthesis and cell mitotic division-related pathways (Fig. 3B). As shown in Fig. 3C, the heat map clearly showed that a number of genes related to DNA replication, including TOP2A, LIG1, and TYMS, as well as genes related to cell mitosis, including AURKB, RRM1, RRM2, and CDC20, were all significantly downregulated by CA treatment. To validate the results of high-throughput sequencing, we designed specific primers and performed RT-qPCR. Figure 3D shows that CCNA2, CCNB1, TOP2A, and LIG1 were significantly downregulated by CA treatment, which was consistent with the high-throughput sequencing results.

Corosolic acid at low concentration inhibited bladder cancer cells via suppression of DNA replication

EdU (5-ethynyl-2'-deoxyuridine) is a substance that can only be incorporated into newly synthesized strands of DNA and is a powerful measure of the DNA synthesis rate. The inhibitory effect of CA on DNA synthesis in bladder cancer cells was evaluated using the EdU method. As shown in Fig. 4A–4D, CA dose-dependently suppressed DNA replication in SW780 and UM-UC-3 bladder cancer cells, which was consistent with the enrichment results of the high-throughput transcriptome sequencing. To further confirm the anti-cancer mechanism of CA, we performed a proteomic assay on CA-treated bladder cancer cells. Then, a combined analysis of the transcriptome and proteome was performed (Fig. 4E). Through

the transcriptome-proteome combined analysis, we found that many genes related to DNA synthesis and mitosis, including CCNA2, CDC20, TOP2A, AURKB, TYMS, RRM1, and RRM2 were downregulated by CA at both mRNA and protein levels. To double confirm the effect of CA on these molecules, immunoblotting and immunofluorescence staining were performed. The effect of CA on CCNA2 protein was verified by cellular immunofluorescence (Fig. 4G). Moreover, the protein alteration caused by CA treatment was analyzed by Western blotting. Figure 4H shows that CCNB1, CCNA2, and RRM2 levels were decreased by CA treatment. The inhibitory effect of CA on cell mitosis-related critical proteins was also verified *in vivo* in mice. Figure 4I and 4J show that CDC20 and RRM2 in subcutaneous tumors of mice treated with CA were significantly reduced compared with those in the control group. The above results strongly indicate that CA inhibits bladder cancer proliferation via the suppression of DNA replication and mitosis.

Corosolic acid at high concentration induced non-apoptotic cell death in bladder cancer cells

During the analysis of morphological changes induced by CA treatment, we found that low concentrations of CA could decrease the growth rate of bladder cancer cells, while high concentrations could cause cell death. Figure 5A shows that the colony formation of bladder cancer cells was significantly inhibited. Notably, high concentration of CA resulted in the failure of cell clone formation and loss of the cells' stretched state, which could be a sign that the cells were predisposed to die. Using flow cytometry, we found that CA significantly reduced the percentage of cell population in the S and G2 phases (Fig. 5B), which verified that the pathways found enriched by multi-omics were rational and correctly identified. It is worth noting that although CA at a concentration of less than 7.0 μg/ml did not induce a significant increase in the subG1 cell population, but a high concentration of CA dramatically increased this population. This result indicates that high concentrations of CA might induce bladder cancer cell death. The calcein-AM/PI double staining results confirmed the above indication that 8.0 μg/ml of CA treatment led to bladder cancer cell death (Fig. 5C). Next, we performed annexin-V/PI double staining to test for apoptosis. As shown in Fig. 5D, CA did not induce apoptosis in bladder cancer cells, suggesting that CA could cause a non-apoptotic cell death mode. Although induction of apoptosis has long been the most common mechanism of anti-cancer agents [22], the discovery of various cell death modes in recent years enables a broader view for screening novel anti-cancer agents [23]. Here, we discovered that CA suppressed bladder cancer cell proliferation at low concentrations and induced non-apoptotic cell death at high concentrations.

Corosolic acid at high concentration induced mitochondrial autophagy

In this study, the mitochondrial autophagy (mitophagy) pathway was found to be enriched by differential protein enrichment analysis (Fig. S1). The heat map in Fig. 6A shows that the mitophagy markers LC3, SQSTM1/p62, NBR1, TAX1BP1, and UBB were upregulated upon CA treatment. We then tested the mitochondrial potential to evaluate mitochondrial damage caused by CA. As shown in Fig. 6B, mitochondrial potential decreased significantly with the increasing doses of CA, which is consistent with

the enrichment analysis results. Since SQSTM1/p62 was reported to be an important mitophagy inducer because of its ability to promote mitochondrial ubiquitination independent of parkin [24], we examined SQSTM1/p62 by immunofluorescence staining. Figure 6C shows that treatment of the cells with high concentrations of CA resulted in the upregulation of SQSTM1/p62, which is an important marker of CA-induced mitophagy. To further verify the induction of mitophagy by CA, LC3 was detected by immunofluorescence staining. As shown in Fig. 6D, with increasing CA concentration, LC3 positive staining was gradually enhanced. Based on the proteomics data and immunofluorescence staining results, we summarized that CA upregulated the autophagy receptor NBR1 and TAX1BP1 which were able to act as an autophagy inducer. Moreover, CA augmented UBB protein level and increased SQSTM1/p62 (a mitophagy marker), in turn leading to LC3 accumulation which marked the onset of autophagy (Fig. 6E).

Discussion

As a natural compound with medicinal value and drug/food homology, CA has recently attracted widespread attentions due to its anticancer effect. Some scholars pointed out that CA inhibited cell proliferation through suppression of STAT3 and NF-κB [25],and some reported that CA promoted cancer cell death through induction of apoptosis via activating caspase − 3, 8 and 9 [26]. But there is a lack of systematic understanding of the anticancer mechanism of CA. Based on multi-omics and multi-perspective analysis, we elucidated a comprehensive understanding on the pharmacological mechanism of CA inhibiting bladder cancer. CA inhibited the proliferation of bladder cancer cells when the concentration of CA was above 5.0μg/ml, and caused cell death when the concentration higher than 7.0μg/ml. 5.0μg/ml ~ 7.0μg/ml CA repressed bladder cancer proliferation was not just achieved by affecting a single protein, but through mitigating many DNA replication and mitosis related proteins (e.g.CCNA2, CCNB1, TOP2A, LIG1 and CDC20). These proteins have been demonstrated as therapeutic targets for many different tumors. *CCNA2*, which is short for cyclin A2, is a regulator of cyclin-dependent kinases that play an important role in cell cycle promotion [27]. The mRNA expression level of CCNA2 in bladder cancer patients was significantly higher than that in the normal population (Fig. 3E), suggesting that CCNA2 may be involved in bladder tumorigenesis. Recently, CCNA2 was considered as a bladder cancer therapy target by Li et al. [28]. The mRNA expression level of CCNB1 in bladder cancer patients was also significantly higher than that in the normal population (Fig. 3E), and CCNB1 has also been reported as a potential target for bladder cancer [29]. In the present study, we found that CA treatment resulted in the downregulation of CCNA2 and CCNB1, which suggests that inhibition of the CCNA2/B1-dependent cell cycle is one of the molecular mechanisms by which CA inhibits bladder cancer. *TOP2A* encodes a DNA topoisomerase, an enzyme that controls and alters the topological states of DNA during transcription [30]. TOP2A is highly expressed in many tumors, including bladder cancer (Fig. 3E), gastric cancer [31], lung cancer [32]and liver cancer [33], and is widely considered as an anti-cancer target molecule [34]. In the present study, TOP2A expression was found to be suppressed by CA treatment, suggesting that repression of DNA replication is a mechanism of CA-inhibition of bladder cancer. *LIG1* also plays an important role in DNA replication, as well as the base excision repair process. Although it

has not been widely considered as an anti-cancer target molecule, many studies have reported that LIG1 abnormalities are associated with multiple tumorigenesis [35]. In this study, we found that CA significantly downregulated LIG1, which may lead to a disruption in DNA synthesis in bladder cancer cells. *CDC20* (cell division cycle protein 20 homolog) is required for two microtubule-dependent processes: nuclear movement prior to anaphase and chromosome separation and chromosome segregation and mitosis [36]. CDC20 is well accepted as a novel therapeutic target for cancer [37]. Figure 3E shows that CDC20 mRNA expression levels in bladder cancer patients were significantly higher than those in the normal population, suggesting that CA might be a potential drug candidate to inhibit bladder cancer tumors by targeting CDC20. *RRM2*, short for ribonucleotide reductase M2, catalyzes the formation of deoxyribonucleotides from ribonucleotides and is a tumor biomarker [38]. Figure 3E shows that the RRM2 mRNA expression level in bladder cancer was significantly higher than that in the normal population. Recently, it was reported that inhibiting RRM2 could enhance the anti-cancer activity of chemotherapy [38], suggesting that CA could be a potent combination drug for chemotherapy, targeting RRM2.

Furthermore, we elucidated that high concentration of CA inhibited the bladder cancer mainly through the up-regulation of TAX1BP1, NBR1, UBB, SQSTM1/P62 and LC3, thus leading to mitochondrial autophagy. TAX1BP1 has been reported to be an autophagy receptor which is recruited and required for the clearance of stress-induced aggregations[39]. NBR1 functions as a specific autophagy receptor for the selective autophagic degradation of peroxisomes, which in turn promotes mitophagy [40]. Besides, NBR1 is involved in cleaning autophagosomes, independently from SQSTM1/p62 [41]. In our study, we found that CA treatment increased TAX1BP1 and NBR1 expression, which would account for the induction of mitophagy. Ubiquitin B (UBB) is one of the major elements for the guidance of cellular protein degradation by the 26S proteasome [42]. Abnormally low expression of UBB has been found in many cancers. The transcriptional inhibition of UBB was found in a large number of women with genital tract cancer [43], and UBB expression is suppressed in approximately 30% of patients with high-grade serous ovarian cancer [43].

Autophagy is a kind of programmed death of eukaryotic cells. Although autophagy was previously thought to play a role in tumor development, Dr. Karlseder demonstrated that the clinical use of autophagy inhibitors did not have a positive effect on cancer patients, but had a tumorigenesis effect. Karlseder pointed out that abnormal DNA replication occurred when cells were stressed or in danger, which is called a "replicative crisis"[44]. Interestingly, cells in replicative crisis tended to die dominantly through autophagy pathway. Karlseder and Nassour discovered that when autophagy was blocked, cells in replicative crisis went crazy and went into a phase of infinite replication. This suggests that autophagy would be an important cancer inhibition mechanism[44]. Consistent to Karlseder’s view, our findings indicate that elevation of autophagy by CA could strongly inhibit bladder cancer cells, which might be a new anticancer strategy.

The graphical abstract in Fig. 7 describes the main mechanisms of CA-inhibition of bladder cancer but does not deny the existence of other mechanisms. For example, as shown in Fig. 3A, CA significantly

upregulated the expression of FBXO32 mRNA. FBXO32 has been shown to be a target gene of TGF-β/Smad4 and plays the role of a tumor suppressor in a variety of tumors [45]. Moreover, the expression of FBXO32 in bladder cancer patients is significantly lower than that in the normal population. FBXO32 is a member of the ubiquitin-protein ligase complex and plays an important role in protein ubiquitination and degradation [45], and it might be responsible for the mitophagy of CA-induced bladder cancer cells. Although the health value of CA has been widely recognized and health food has been developed due to its ability to lower blood sugar and anti-inflammatory properties [46, 47], there is still a lack of studies on its anti-tumor activities. In particular, there is a need for studies revealing the comprehensive molecular mechanism of the CA biological activities based on multi-omics analysis.

Conclusions

Our study discovered the inhibitory effect of CA on bladder cancer using cell and animal model. Through combined transcriptome and proteomics study, we analyzed the underlying anti-cancer mechanisms of CA from a comprehensive perspective and revealed that low concentration of CA inhibited proliferation of cancer cells by repressing DNA replication and restricting cell mitosis through the suppression of LIG1, TOP2A, CCNA2, CCNB1, CDC20, RRM2 and so on, while high concentrations of CA induced mitophagy of bladder cancer cells through upregulation of SQSTM1/P62, NBR1, and UBB (Fig. 7). This study provides comprehensive insights into the pharmacological mechanisms of CA in inhibiting bladder cancer, which would be helpful in developing new anti-tumor drugs based on CA.

Abbreviations

CA
corosolic acid; FBS:Fetal Bovine Serum; EdU:5-ethynyl-2'-deoxyuridine; PI:propidium iodide; H&E staining:hematoxylin-eosin staining; IHC:Immunohistochemistry; IF:Immunofluorescence.

Declarations

Ethics approval and consent to participate

The whole protocols were approved by the Ethics Committee of Jining Medical University, China.

Consent for publication

All the authors consent for this manuscript publication.

Availability of data and materials

The transcriptome data are uploaded on NCBI Sequence Read Archive and available via http://www.ncbi.nlm.nih.gov/bioproject/739015 (BioProject ID: PRJNA739015). The mass spectrometry proteomics data have been deposited to the ProteomeXchange Consortium

(http://proteomecentral.proteomexchange.org) via the iProX partner repository with the dataset identifier PXD026919. The other data are available in the main text or the supplementary materials.

Competing interests

The authors declare no potential conflicts of interest.

Funding

Taishan Scholars Program of Shandong Province (Grant No.tsqn201909147), National Nature Science Foundation of China (Grant No. 81873854, No. 82000761), The Research Fund for Academician Lin He New Medicine (Grant No.JYHL2019ZD01), Teachers' Research Support Fund of Jining Medical University (No. JYFC2019KJ031) and Project of Shandong Province Higher Educational Science and Technology Program (No. J17KB086).

Author contributions

YX and FP designed and supervised the study, AC, XL and XM performed biological experiments, and PL collected the clinical data for patients. YX and ZS performed bioinformatics or database analysis. XL, XW and CL helped analyze the data. YX drafted the manuscript. XW and CL helped the animal studies. FP and AC helped edit the manuscript. All authors approved the final manuscript**.**

Author contributions

Not applicable

References

1. Lenis AT, Lec PM, Chamie K. Bladder Cancer: A Review. Jama-Journal of the American Medical Association. 2020;324(19):1980–91.
2. Richters A, Aben KKH, Kiemeney LALM. The global burden of urinary bladder cancer: an update. World J Urol. 2020;38(8):1895–904.
3. Redelman-Sidi G, Glickman MS, Bochner BH. The mechanism of action of BCG therapy for bladder cancer-a current perspective. Nature Reviews Urology. 2014;11(3):153–62.
4. Kates M, et al. Adaptive Immune Resistance to Intravesical BCG in Non-Muscle Invasive Bladder Cancer: Implications for Prospective BCG-Unresponsive Trials. Clin Cancer Res. 2020;26(4):882–91.
5. Asin MAPJ, et al. Bacillus Calmette-Guerin (BCG) Infection Following Intravesical BCG Administration as Adjunctive Therapy For Bladder Cancer Incidence, Risk Factors, and Outcome in a Single-Institution Series and Review of the Literature. Medicine. 2014;93(17):236–54.
6. Green DB, et al. Complications of Intravesical BCG Immunotherapy for Bladder Cancer. Radiographics. 2019;39(1):80–94.

7. Marques M, et al. Disseminated Bacillus Calmette-Guerin (BCG) infection with pulmonary and renal involvement: A rare complication of BCG immunotherapy. A case report and narrative review. Pulmonology. 2020;26(6):346–52.
8. Kijima T, et al. Selective tetramodal bladder-preservation therapy, incorporating induction chemoradiotherapy and consolidative partial cystectomy with pelvic lymph node dissection for muscle-invasive bladder cancer: oncological and functional outcomes of 107 patients. Bju International. 2019;124(2):242–50.
9. Chikara S, et al. Oxidative stress and dietary phytochemicals: Role in cancer chemoprevention and treatment. Cancer Lett. 2018;413:122–34.
10. Rauf A, et al. Resveratrol as an anti-cancer agent: A review. Crit Rev Food Sci Nutr. 2018;58(9):1428–47.
11. Bernatoniene J, Kopustinskiene DM. *The Role of Catechins in Cellular Responses to Oxidative Stress*. Molecules, 2018. 23(4).
12. Weaver BA. How Taxol/paclitaxel kills cancer cells. Mol Biol Cell. 2014;25(18):2677–81.
13. Guo X, et al. Reduced Lipocalin 2 Expression Contributes to Vincristine Resistance in Human Colon Cancer Cells. Recent Pat Anti-Cancer Drug Discovery. 2018;13(2):248–54.
14. Feng X, et al. Microbial transformation of the anti-diabetic agent corosolic acid by Cunninghamella echinulata. J Asian Nat Prod Res. 2017;19(7):645–50.
15. Li XQ, et al. Cell-penetrating corosolic acid liposome as a functional carrier for delivering chemotherapeutic drugs. Acta Biomater. 2020;106:301–13.
16. Zhang BY, et al., *Study on the absorption of corosolic acid in the gastrointestinal tract and its metabolites in rats*. Toxicology and Applied Pharmacology, 2019. 378.
17. Yang J, et al. Corosolic acid inhibits adipose tissue inflammation and ameliorates insulin resistance via AMPK activation in high-fat fed mice. Phytomedicine. 2016;23(2):181–90.
18. Sivakumar G, et al. Plant-based corosolic acid: future anti-diabetic drug? Biotechnol J. 2009;4(12):1704–11.
19. Zhang BY, et al. Corosolic acid inhibits colorectal cancer cells growth as a novel HER2/HER3 heterodimerization inhibitor. Br J Pharmacol. 2021;178(6):1475–91.
20. Wang K, et al. Corosolic acid induces cell cycle arrest and cell apoptosis in human retinoblastoma Y-79 cells via disruption of MELK-FoxM1 signaling. Oncol Rep. 2018;39(6):2777–86.
21. Yang J, et al. The triterpenoid corosolic acid blocks transformation and epigenetically reactivates Nrf2 in TRAMP-C1 prostate cells. Mol Carcinog. 2018;57(4):512–21.
22. Ismail MMF, et al., *Apoptosis: A target for anticancer therapy with novel cyanopyridines*. Bioorganic Chemistry, 2020. 94.
23. Miyazawa S, et al. Vitamin K-2 induces non-apoptotic cell death along with autophagosome formation in breast cancer cell lines. Breast Cancer. 2020;27(2):225–35.

24. Yamada T, et al. SQSTM1/p62 promotes mitochondrial ubiquitination independently of PINK1 and PRKN/parkin in mitophagy. Autophagy. 2019;15(11):2012–8.
25. Fujiwara Y, et al. Corosolic acid inhibits glioblastoma cell proliferation by suppressing the activation of signal transducer and activator of transcription-3 and nuclear factor-kappa B in tumor cells and tumor-associated macrophages. Cancer Sci. 2011;102(1):206–11.
26. Cai XB, et al. Corosolic Acid Triggers Mitochondria and Caspase-dependent Apoptotic Cell Death in Osteosarcoma MG-63 Cells. Phytother Res. 2011;25(9):1354–61.
27. Bayard Q, et al., *Cyclin A2/E1 activation defines a hepatocellular carcinoma subclass with a rearrangement signature of replication stress*. Nature Communications, 2018. 9.
28. Li JF, et al. Dual regulatory role of CCNA2 in modulating CDK6 and MET-mediated cell-cycle pathway and EMT progression is blocked by miR-381-3p in bladder cancer. Faseb Journal. 2019;33(1):1374–88.
29. Liu AW, et al. Overexpression of G2 and S phase-expressed-1 contributes to cell proliferation, migration, and invasion via regulating p53/FoxM1/CCNB1 pathway and predicts poor prognosis in bladder cancer. Int J Biol Macromol. 2019;123:322–34.
30. Jain M, et al. TOP2A is overexpressed and is a therapeutic target for adrenocortical carcinoma. Endocr Relat Cancer. 2013;20(3):361–70.
31. Hou GX, et al., *Mining topoisomerase isoforms in gastric cancer*. Gene, 2020. 754.
32. Ma WX, et al., *Prognostic significance of TOP2A in non-small cell lung cancer revealed by bioinformatic analysis*. Cancer Cell International, 2019. 19(1).
33. Panvichian R, et al., *TOP2A Amplification and Overexpression in Hepatocellular Carcinoma Tissues.* Biomed Research International, 2015. **2015**.
34. Delgado JL, et al. Topoisomerases as anticancer targets. Biochem J. 2018;475:373–98.
35. Martinez-Terroba E, et al. The oncogenic RNA-binding protein SRSF1 regulates LIG1 in non-small cell lung cancer. Lab Invest. 2018;98(12):1562–74.
36. Kapanidou M, Curtis NL, Bolanos-Garcia VM, *Ccc20: At the Crossroads between Chromosome Segregation and Mitotic Exit.* Trends in Biochemical Sciences, 2017. **42**(3): p. 193–205.
37. Wang LX, et al. Targeting Cdc20 as a novel cancer therapeutic strategy. Pharmacol Ther. 2015;151:141–51.
38. Yang YY, et al., *RRM2 protects against ferroptosis and is a tumor biomarker for liver cancer*. Cancer Cell International, 2020. 20(1).
39. Sarraf SA, et al., *Loss of TAX1BP1-Directed Autophagy Results in Protein Aggregate Accumulation in the Brain*. Molecular Cell, 2020. 80(5).
40. Shi J, et al. NBR1 is dispensable for PARK2-mediated mitophagy regardless of the presence or absence of SQSTM1. 6: Cell Death & Disease; 2015.
41. Vainshtein A, Grumati P. *Selective Autophagy by Close Encounters of the Ubiquitin Kind.* Cells, 2020. 9(11).

42. Chen RH, Chen YH, Huang TY. *Ubiquitin-mediated regulation of autophagy*. Journal of Biomedical Science, 2019. 26(1).
43. Kedves AT, et al. Recurrent ubiquitin B silencing in gynecological cancers establishes dependence on ubiquitin C. Journal of Clinical Investigation. 2017;127(12):4554–68.
44. Nassour J, et al. Autophagic cell death restricts chromosomal instability during replicative crisis. Nature. 2019;565(7741):659-+.
45. Zhou H, et al. FBXO32 suppresses breast cancer tumorigenesis through targeting KLF4 to proteasomal degradation. Oncogene. 2017;36(23):3312–21.
46. Caligiani A, et al. A simple GC-MS method for the screening of betulinic, corosolic, maslinic, oleanolic and ursolic acid contents in commercial botanicals used as food supplement ingredients. Food Chem. 2013;136(2):735–41.
47. Shi L, et al. Corosolic acid stimulates glucose uptake via enhancing insulin receptor phosphorylation. Eur J Pharmacol. 2008;584(1):21–9.

Figures

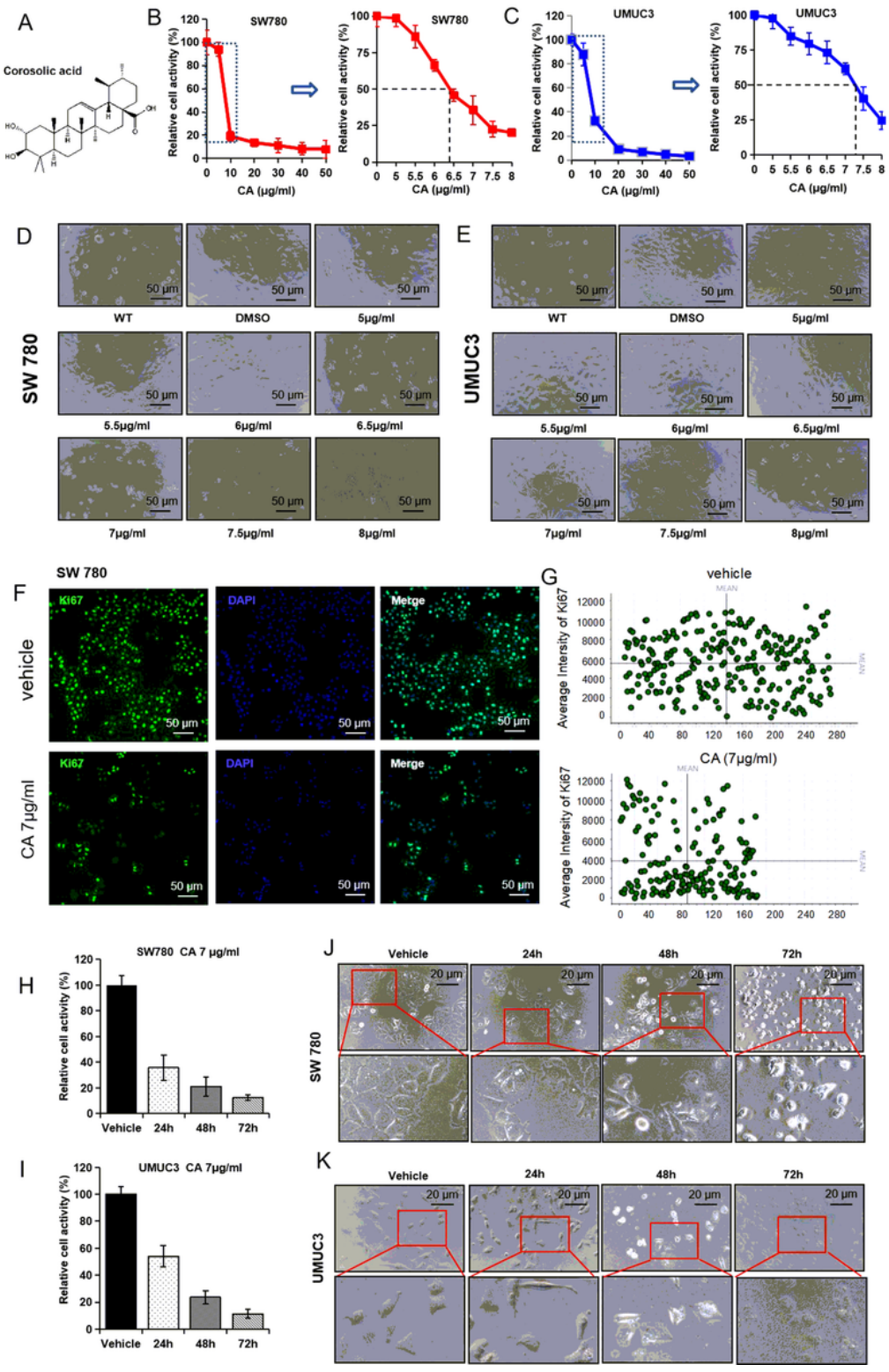

Figure 1

CA inhibited bladder cancer cells in dose-dependent and time-dependent manner in vitro. (A) The formula of corosolic acid; (B) Bladder cancer SW780 cells was co-incubate in different concentration of CA for 24h, and the cell activity was detected by CCK8 kit; (C) Bladder cancer UMUC3 cells were co-incubated in different concentration of CA for 24h, and the cell activity was detected by CCK8 kit. (D) Bladder cancer SW780 cells were co-incubated in different concentration of CA for 24h, and the morphological photos

were recorded by a microscope. (E) Bladder cancer UMUC3 cells were co-incubated in different concentration of CA for 24h, and the morphological photos were recorded by a microscope. (F) Bladder cancer SW780 cells were co-incubated in 7.0 μg/ml CA for 24h, and the ki67 was detected by immunofluorescence staining. (G) The average intensity of ki67 fluorescence was quantitated (Data were from same experiments with F). (H) CA reduced SW780 cell activity in a time-dependent manner. (I) CA reduced UMUC3 cell activity in a time-dependent manner. (J) CA caused the morphological alteration of SW780 cells. (K) CA caused the morphological alteration of UMUC3 cells.

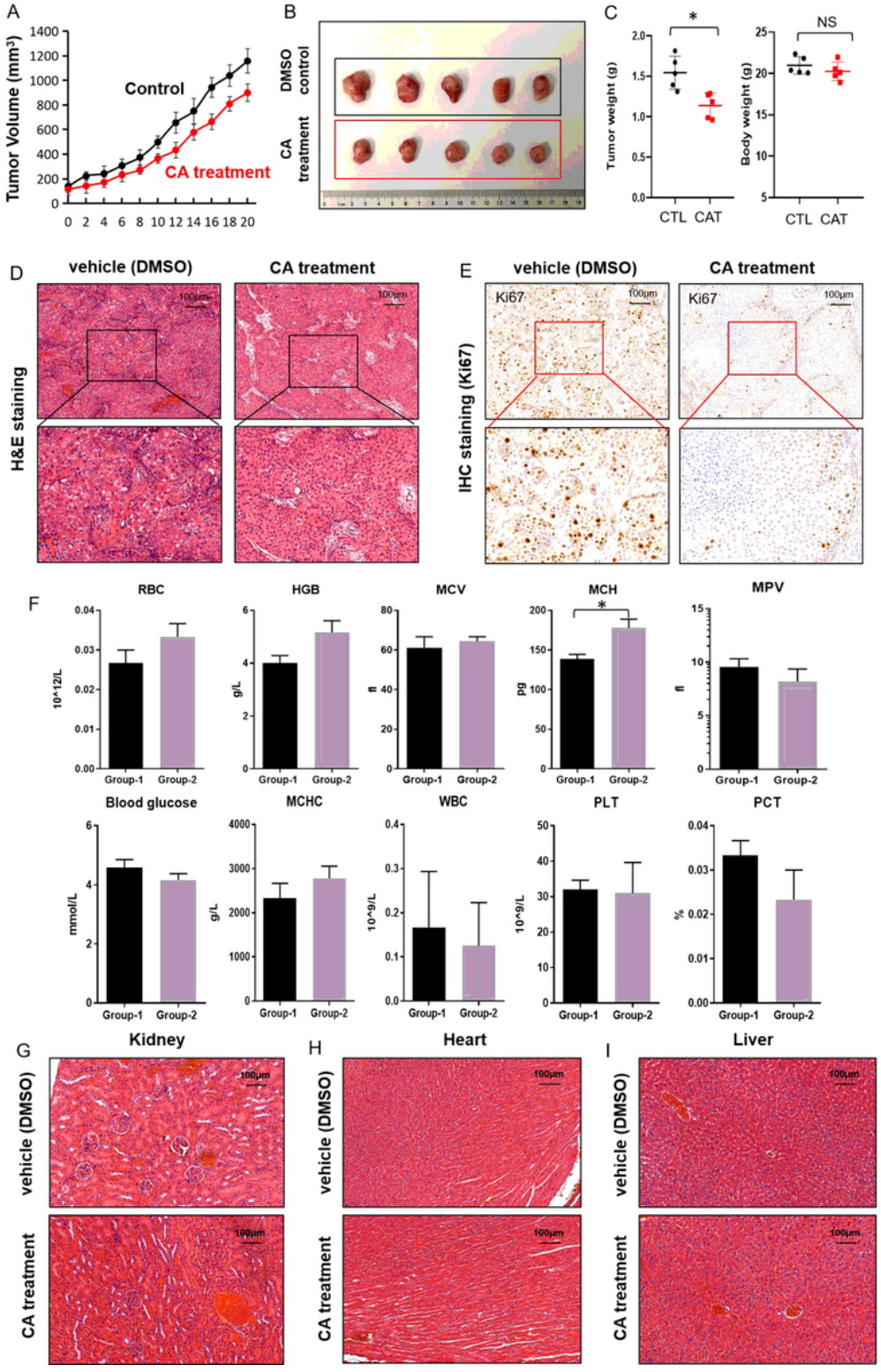

Figure 2

CA suppressed transplanted bladder tumor in vivo. (A) The tumor size was recorded after the mice began to be treated by CA or vehicle. (B) After the mice were sacrificed, tumors were isolated and taken photos. (C) The mice body weight and tumors weight was compared, the difference significance was calculated by two-way t-test, * $p<0.05$. (D) H&E staining of xenograft tumor with different magnificence. (E) Proliferation marker Ki67 was stained by IHC, and the photos with different magnificence were shown. (F) The blood routine index and blood glucose was detected. The difference significance between two groups was calculated by two-way t-test, * $p<0.05$. (G) The H&E staining results of renal sections of the CA-treated group and the control group. (H) The H&E staining results of heart sections of the CA-treated group and the control group. (I) The H&E staining results of liver sections of the CA-treated group and the control group.

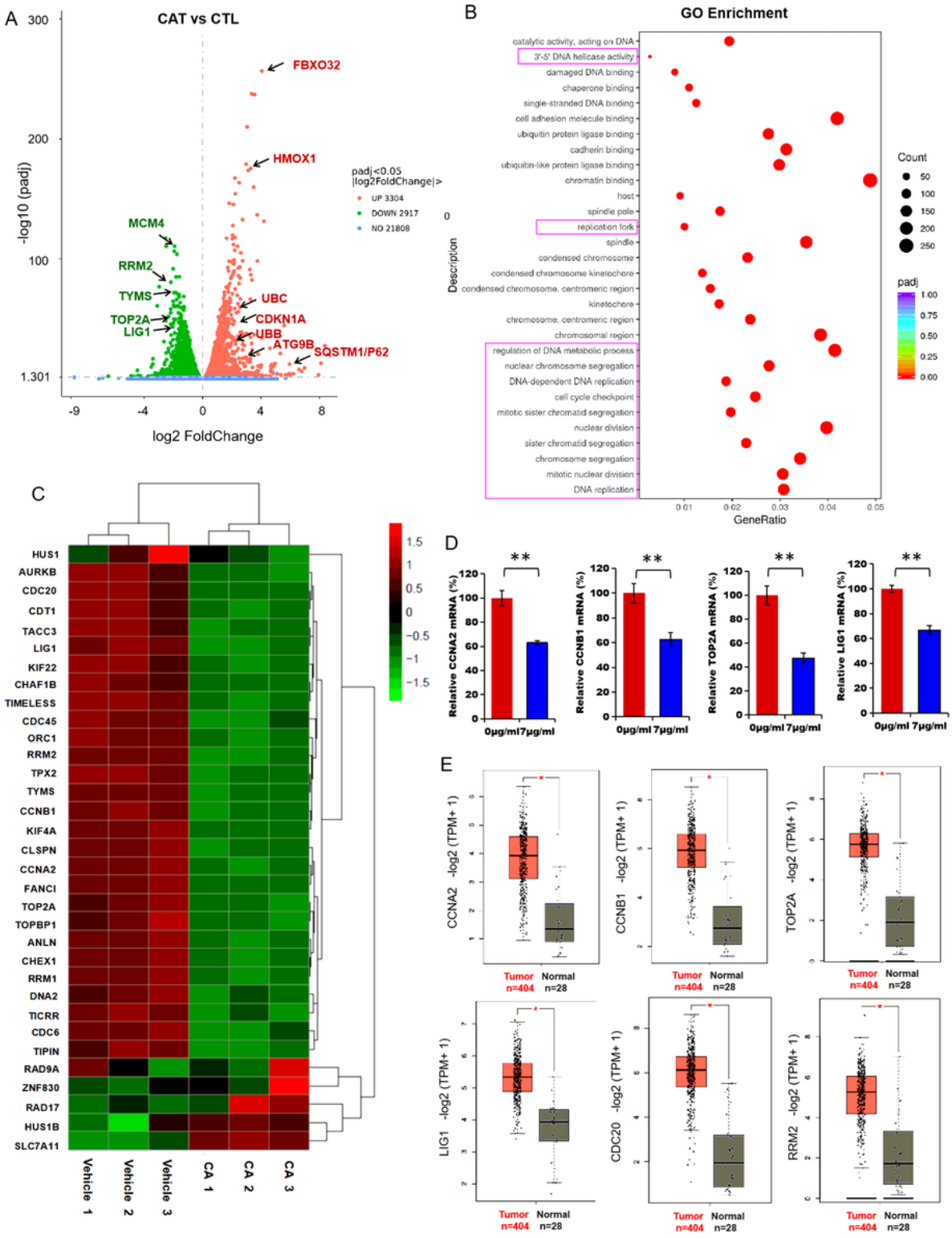

Figure 3

Transcriptomics result indicated that CA suppressed DNA synthesis and cell division. (A) Volcanic map of different genes between CA treatment group and control group. CAT represents CA treatment; CTL represents vehicle (DMSO) treatment. (B) GO enrichment result of different genes between treatment group and control group. The red squares represent the pathways related to DNA replication and cell division. (C) The heatmap of the genes with significant difference related to DNA replication and cell

division. (D) The mRNA level of CCNA2, CCNB1, TOP2A and LIG1 was detected by RT-qPCR. Every test was repeated three times. The difference was calculated by two-way t-test, ** p<0.01. (E) The expression of CCNA2, CCNB1, TOP2A, CDC20, RRM2 and LIG1 in normal bladder tissue and clinical bladder tumor tissue (Data are from TCGA database). Red column represents tumor tissue, and gray column represents normal tissue. The statistical analysis was performed by ANOVA, * p<0.05.

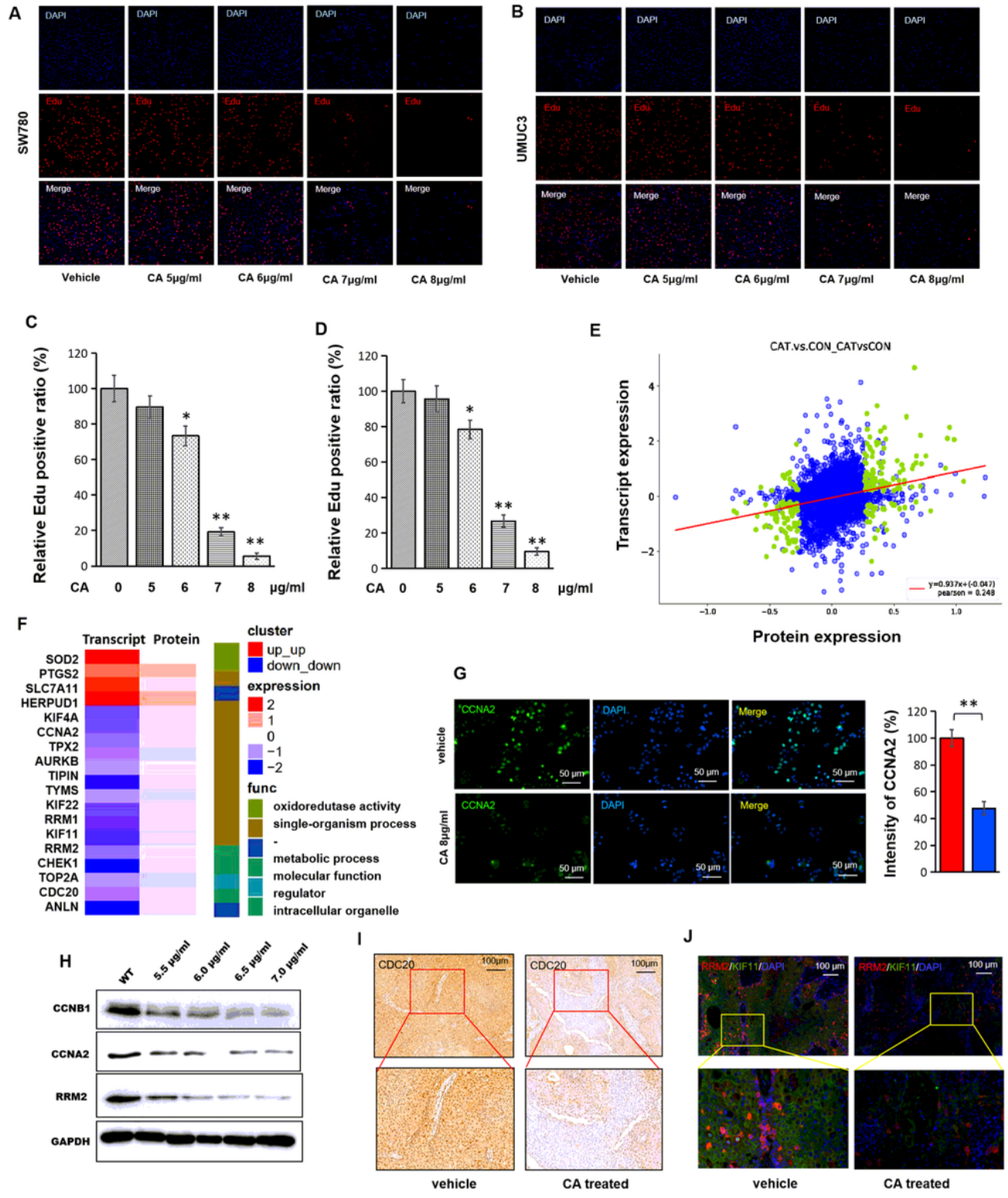

Figure 4

Experimental evidence of CA inhibited bladder cancer cells by inhibiting DNA synthesis and cell mitosis. (A) The DNA synthesis speed was detected by EdU staining in SW780 cells. (B) The DNA synthesis speed was detected by EdU staining in UMUC3 cells. (C) The relative DNA synthesis speed in SW780 was calculated. The difference was calculated by two-way t-test, * $p<0.05$, ** $p<0.01$. (D) The relative DNA synthesis speed in UMUC3 was calculated. The difference was calculated by two-way t-test, * $p<0.05$, ** $p<0.01$. (E) Combined analysis of transcriptome and proteome: the protein and mRNA expression correlate with the same expression trend. (F) Combined analysis for DNA synthesis related molecules in both mRNA level and protein level. (G) CCNA2 was detected by immunofluorescence staining. The fluorescence intensity of CCNA2 was measured by ImageJ, the comparison of CCNA2 fluorescence intensity was shown in column figure (right). The difference was calculated by two-way t-test, ** $p<0.01$. (H) The CCNB1, CCNA2, RRM2 and GAPDH were tested by western blotting. (I) The CDC20 level in CA treated xenograft tumors were tested by IHC staining. The two lower images are magnified version of the upper ones. (J) The RRM2 and KIF11 were detected in CA treated xenograft tumors were tested by IF staining. The two lower images are magnified version of the upper ones.

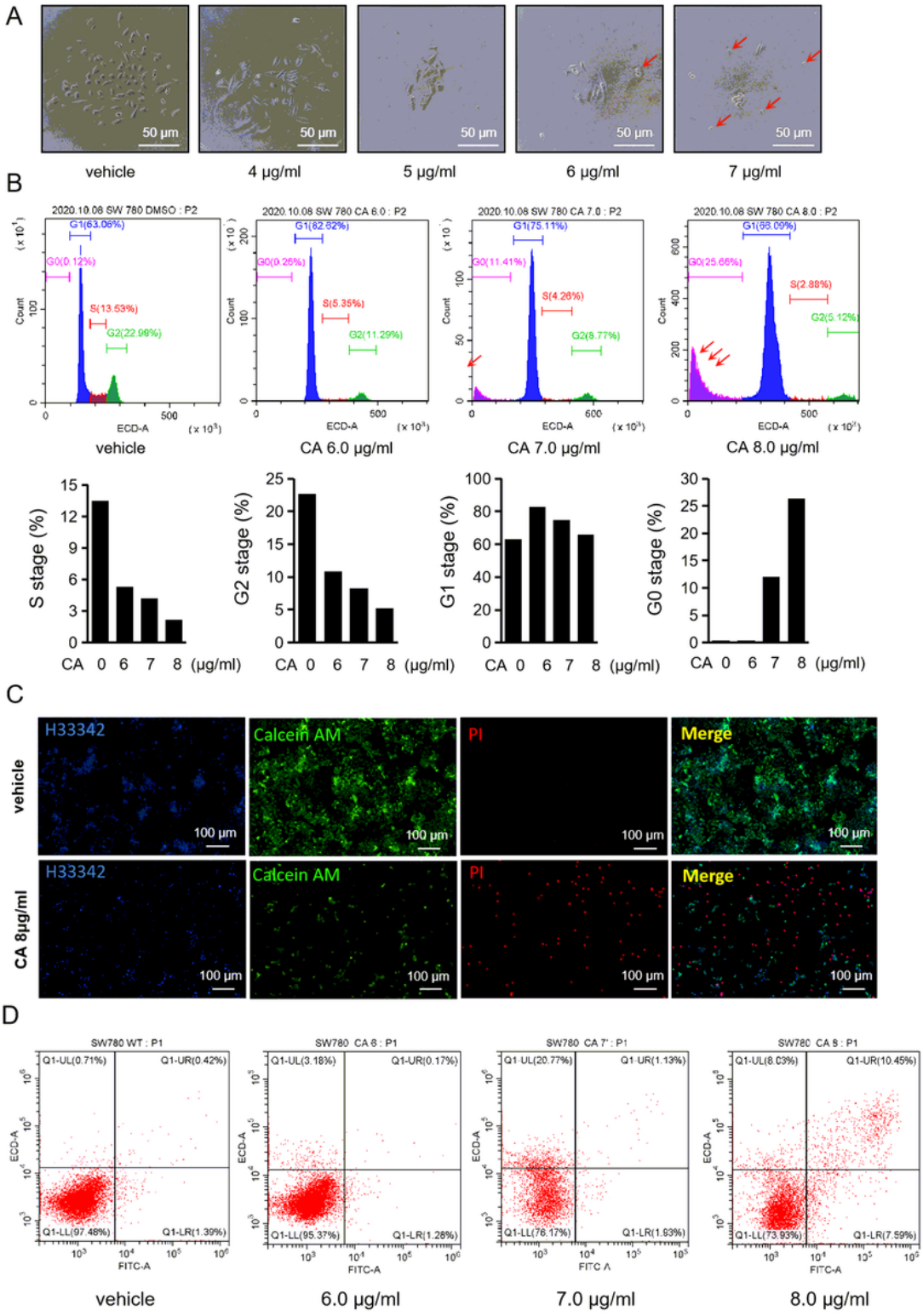

Figure 5

CA induced bladder cancer cell death in a non-apoptotic manner. (A) Bladder cancer cells were co-incubated with different concentration of CA, and the morphological alteration was recorded by a microscope. Note: as the red arrows showed, with the CA concentration lower than 6 μg/ml, bladder cancer cells growth speed decreased; while the CA concentration higher than 6 μg/ml, the cell morphology changed obviously (marked by red arrows). (B) The CA treated bladder cancer cells were

stained by PI, and flow cytometry was employed to detect the cell cycle. The comparison of each stage was shown in the lower figure (column figure). The red arrow indicated impaired cells. (C) The DMSO or CA treated cells were triple stained by calcein AM / PI / H33342 to examine the cell death. H33342 stained cells were shown in blue, calceim AM stained cells were shown in green, and PI stained cells were shown in Red. (D) The cells were double stained by Annix-V-FITC / PI, and the flow cytometry was used for testing the apoptosis. Note: as shown in Fig.5D, the CA induced bladder cancer cell death by a non-apoptotic manner.

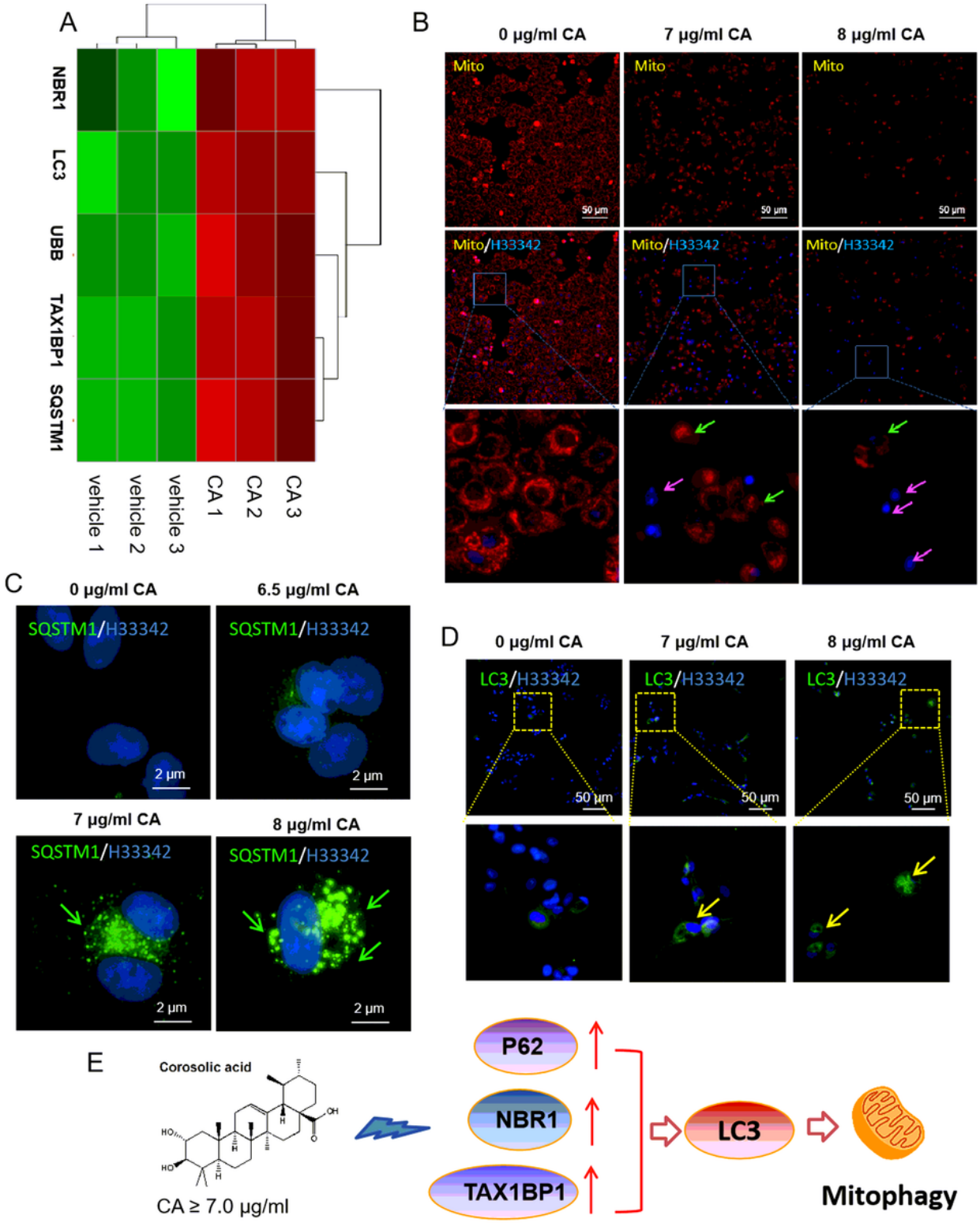

Figure 6

CA induced bladder cancer cell death via inducing mitophagy. (A) Enrichment analysis of proteomic results showed that CA up-regulated the elevation of a variety of mitophagy related proteins such as NBR1, LC3, UBB, TAXBP1 and SQSTM1/p62. Red represented increased protein, and green represented decreased protein. (B) The effect of CA on the mitochondrial membrane potential of bladder cancer cells was detected by Mito-Tracker Red CMXRos kit. The intensity of the red color is proportional to the mitochondrial membrane potential. CA reduced mitochondrial membrane potential in a concentration-dependent manner. The green arrows represented cells with decreased mitochondrial membrane potential, while the purple arrows represented cells with lost mitochondrial membrane potential, suggesting that CA might cause mitochondrial depletion. (C) The effect of CA on SQSTM1/p62 was determined by immunofluorescence. The SQSTM1/p62 was stained by green and H33342 was blue. Note: 6.5 μg/ml CA can only induce feeble SQSTM1/p62, CA with concentration higher than 7.0 μg/ml strongly elevated SQSTM1/p62 in bladder cancer cells. (D) Autophagy marker LC3 was examined by IF staining. The results showed CA induced LC3 in a dose-dependent manner. (E) A concise mechanic diagram of CA caused mitophagy by elevating SQSTM1/p62, NBR1 and TAXBP1.

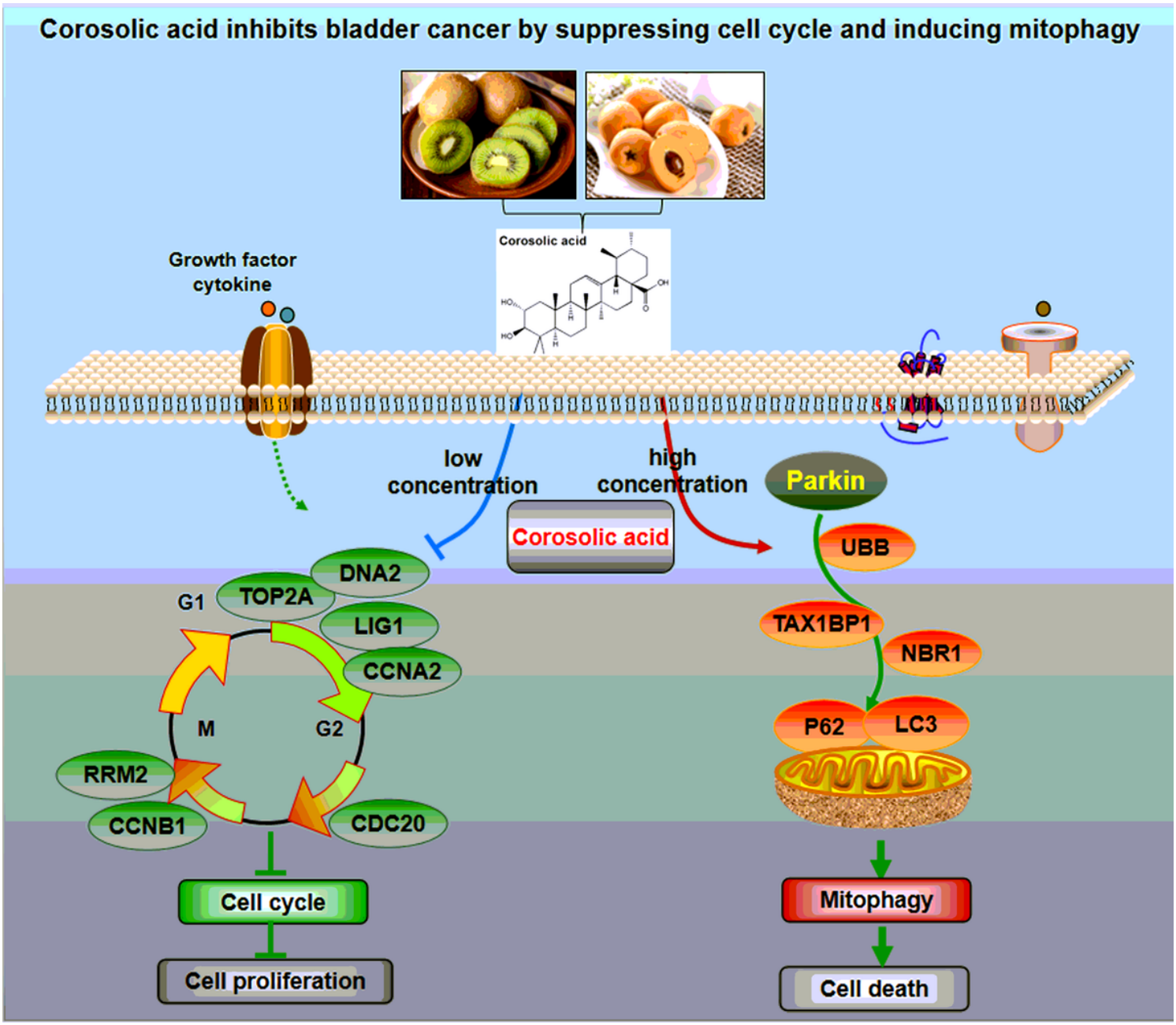

Figure 7

Summary diagram of the molecular mechanisms by which CA inhibits bladder cancer. CA inhibits bladder cancer cells through different mechanisms at low and high concentrations: low concentration of CA inhibited the proliferation of bladder cancer cells by down-regulation of TOP2A, LIG1, CCNA2, CCNB1, RRM2 and CDC20 to inhibit DNA replication and cell mitosis; while high concentration of CA led to cell death of bladder cancer cells via induction of mitophagy through increasing UBB, TAX1BP1, NBR1, SQSTM1/p62 and LC3.

Supplementary Files

This is a list of supplementary files associated with this preprint. Click to download.

- S1.tif